



TITLE:

Stability improvement of photovoltaic performance in antimony sulfide-based hybrid solar cells

AUTHOR(S):

Hayakawa, Akinobu; Yukawa, Mayumi; Sagawa, Takashi

CITATION:

Hayakawa, Akinobu ...[et al]. Stability improvement of photovoltaic performance in antimony sulfide-based hybrid solar cells. ECS Journal of Solid State Science and Technology 2017, 6(4): Q35-Q38

ISSUE DATE:

2017-02-03

URL:

<http://hdl.handle.net/2433/235558>

RIGHT:

© The Author(s) 2017. Published by ECS. This is an open access article distributed under the terms of the Creative Commons Attribution 4.0 License (CC BY, <http://creativecommons.org/licenses/by/4.0/>), which permits unrestricted reuse of the work in any medium, provided the original work is properly cited.



Stability Improvement of Photovoltaic Performance in Antimony Sulfide-Based Hybrid Solar Cells

Akinobu Hayakawa,^{a,b} Mayumi Yukawa,^{a,b} and Takashi Sagawa^{a,*}

^aGraduate School of Energy Science, Kyoto University, Kyoto 606-8501, Japan

^bSekisui Chemical Co., Ltd., Shimamoto, Osaka 618-0021, Japan

Sb₂S₃-based hybrid solar cells were prepared in the combination with electron transporting layer of TiO₂ or ZnO nanoparticles in addition to poly(3-hexylthiophene)-2,5-diyl/(3, 4-ethylenedioxythiophene): poly(styrene sulfonate), zinc phthalocyanine (ZnPc), or MoO₃ for hole transporting layer. Photovoltaic performance and durability of the hybrid solar cells were compared each other with or without encapsulation by using glass and UV cutoff film. Among these hybrid solar cells, it was found that a combination of glass-ITO/TiO₂/Sb₂S₃/ZnPc/Au encapsulated with glass and UV cut filter has the highest durability with keeping the relative power conversion efficiency of 90% through the stability test under 1 sun at 63°C at a relative humidity of 50% for 1,500 h.

© The Author(s) 2017. Published by ECS. This is an open access article distributed under the terms of the Creative Commons Attribution 4.0 License (CC BY, <http://creativecommons.org/licenses/by/4.0/>), which permits unrestricted reuse of the work in any medium, provided the original work is properly cited. [DOI: 10.1149/2.0101704jss] All rights reserved.



Manuscript submitted November 21, 2016; revised manuscript received January 3, 2017. Published February 3, 2017. This was Paper 804 presented at the San Diego, California, Meeting of the Society, May 29- June 2, 2016.

Various materials such as antimony sulfide (Sb₂S₃),¹⁻⁴ antimony selenide,⁵ lead sulfide,⁶ cadmium selenide,⁷ lead-halogen perovskite⁸⁻¹⁰ have recently been applied for organic-inorganic hybrid solar cells. Among these materials, Sb₂S₃ has much attraction for photovoltaics in terms of appropriate bandgap, high absorption coefficient, low toxicity, and abundance.¹¹ Sb₂S₃ has been prepared by chemical bath deposition,¹⁻⁴ atomic layer deposition,¹² complex-decomposition method,¹³ and so on and applied as the thin film for solar cell, which has been attained the power conversion efficiency (*PCE*) of 7.5%.⁴ Although Sb₂S₃-based solar cell seems to be stable in air,^{1,14} stability test under the accelerated conditions has not yet been reported. In addition, various materials such as TiO₂,¹ ZnO,¹⁵⁻¹⁸ or SnO₂¹⁹ have been utilized as an electron transporting layer (ETL) and polythiophenes,¹⁻⁴ 2,2',7,7'-tetrakis(*N,N*-di-*p*-methoxyphenylamine)-9,9'-spirobifluorene,²⁰ ZnPc, CuSCN,²¹ MoO₃,²² or NiO²³ have been used as a hole transporting layer (HTL) of the Sb₂S₃ based solar cells, however, optimization of the combinations of ETL and HTL in terms of the durability has also not yet been explored. In this context, we prepared Sb₂S₃-based solar cells with TiO₂ or ZnO nanoparticles for ETL in addition to poly(3-hexylthiophene)-2,5-diyl (P3HT)/ (3, 4-ethylenedioxythiophene):poly(styrene sulfonate) (PEDOT: PSS), ZnPc, or MoO₃ for HTL and compared their photovoltaic properties with encapsulation by using glass and UV cutoff films under JIS C8938 conditions of 1 sun at 63°C at a relative humidity (RH) of 50%.

Experimental

Preparation of TiO₂ nanoparticle.—A 14.7 g of TiO₂ powder P-90 (Degussa, Evonic Japan Co., Ltd.) was dispersed in 62.3 g of 95% ethanol. After addition of 439 g of zirconia beads (φ 50 μm), the TiO₂ powder was ground with beads mill at 2000 rpm for 2 h. After the removal of the zirconia beads by filtration, ca. 60 g of TiO₂ slurry was obtained. Addition of adjusted amount of ethanol into the above TiO₂ sludge resulted in 6 wt% TiO₂-dispersed solution.

Preparation of ZnO nanoparticle.—ZnO nanoparticles were prepared according to the reported procedures²⁴ with slight modifications. Zinc acetate dihydrate (0.298 g) was dissolved in methanol (10 g) and stirred for 3 min with heating up to 65°C. 5 g of 3 wt% KOH in methanol was poured into the above solution and stirred for 2.5 h. After centrifugation at 20,000 rpm for 15 min and the removal of the supernatant, the crude precipitates were dispersed in 150 g of methanol through sonication. Thereafter, following another centrifugation at 20,000 rpm for 30 min and the removal of the supernatant,

the purified precipitates were homogeneously dispersed again in 0.5 g of CHCl₃ as ZnO nanoparticles with an average diameter of ca. 5 nm, as confirmed by TEM observation. Methanol was added to the above ZnO-dispersed solution and adjusted to 2 wt%.

Preparation of Sb₂S₃-based hybrid solar cells.—In the preparation of solar cell devices, indium-tin oxide (ITO)-coated glass substrates (Geomatec, 10 Ω cm⁻²) were spin coated with the above dispersed solution of TiO₂ or ZnO at 4,000 rpm followed by annealing at 300°C for 10 min with a hot-plate. A ~100-nm-thick Sb₂S₃ was deposited by thermal evaporation of the Sb₂S₃-powder as the source under vacuum (5 × 10⁻² Pa) onto the metal oxide layer. It was annealed at 260°C for 10 min ramping from 220°C under the reduced pressure (1 × 10² Pa). After cooling down to 220°C, HTL was subsequently coated onto the Sb₂S₃ layer as follows. 0.5 wt% P3HT in chlorobenzene was spin-coated at 4,000 rpm and 3 times diluted PEDOT:PSS solution (Clevios P) with methanol was then coated at 2,500 rpm followed by annealing at 110°C for 10 min. While ZnPc or MoO₃ was deposited by thermal evaporation resulting in a 20-nm-thick layer. Thereafter Au electrode was deposited by thermal evaporation.

The solar cells obtained as described above were encapsulated with glass and epoxy resin as sealer. A cut filter (> 420 nm, Asahi Spectra Co.,Ltd) was utilized for cut off the UV region of the irradiation light.

Evaluations of photovoltaic performance.—Photovoltaic characteristics were measured under AM1.5 (100 mW cm⁻²) with solar simulator of HAL-320 (Asahi Spectra Co., Ltd.) in the combination with COSMO CIV-1000F applying a bias from -0.2 to 1.0 V in steps of 0.05 V and the current density was measured just after 0.5 s under biased conditions.

Results and Discussion

Photovoltaic performance of the Sb₂S₃-based hybrid solar cells for 1 d.—The photovoltaic performance of the Sb₂S₃-based hybrid solar cells with three different HTLs consisting of glass-ITO/TiO₂/Sb₂S₃/HTL (HTL = P3HT/PEDOT: PSS, ZnPc, or MoO₃)/Au were prepared and compared with each other. The current density-voltage (*J*-*V*) curves of the initial (*viz.*, freshly prepared) photovoltaic performance (solid) and the curves after 1 d at 63°C and 50% RH in the dark (broken) are shown in Figure 1. *PCEs* of ca. 3% were attained with P3HT/PEDOT: PSS and ZnPc. While *PCE* of 0.25% was obtained when MoO₃ was applied. Since relatively higher series resistance was observed in the case of MoO₃, it might be estimated that the mobility in MoO₃ is lower than other HTLs and resulted in low *PCE*. With regard to the stability, the *PCE* of P3HT/PEDOT: PSS decreased slightly after 1 d at 63°C and 50% RH even when there was

*Electrochemical Society Member.

^zE-mail: sagawa@energy.kyoto-u.ac.jp

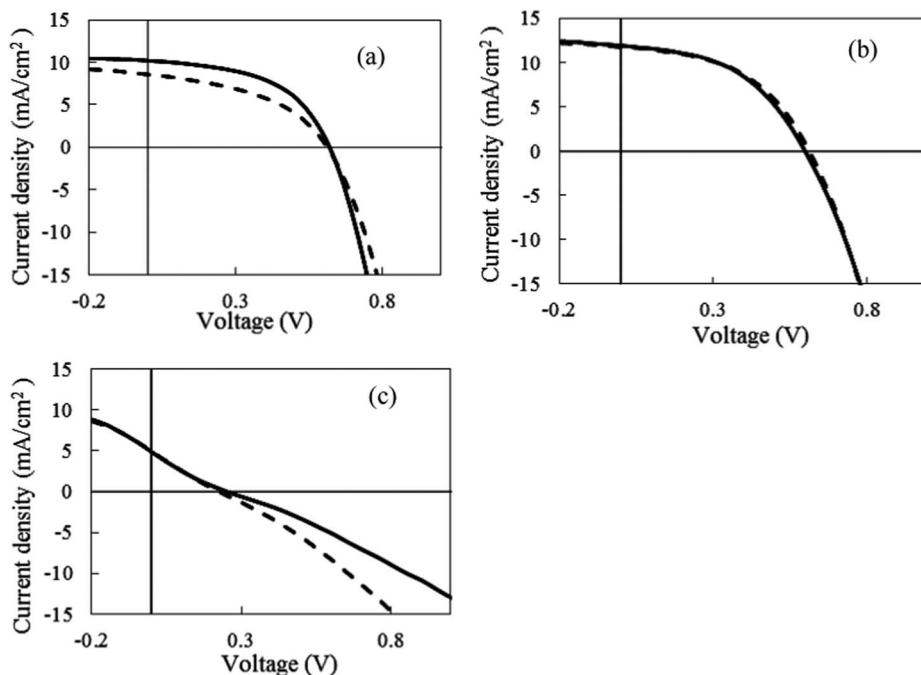


Figure 1. *J-V* curves of (a) glass-ITO/TiO₂/Sb₂S₃/P3HT/PEDOT:PSS/Au, (b) glass-ITO/TiO₂/Sb₂S₃/ZnPc/Au, and (c) glass-ITO/TiO₂/Sb₂S₃/MoO₃/Au fresh after preparation (solid), and after 1 d storage at 63°C and 50% RH in the dark (broken).

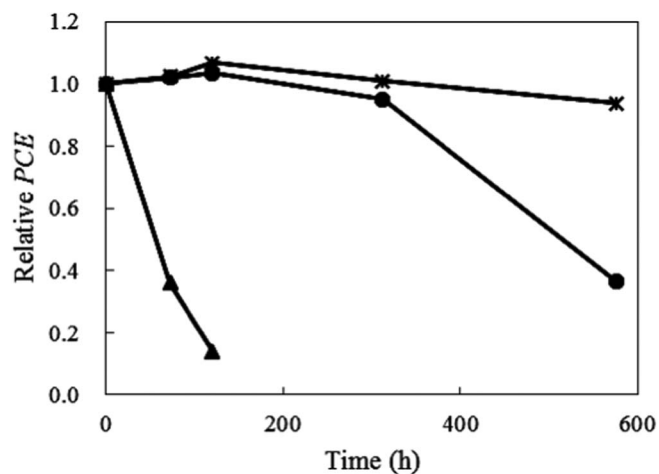


Figure 2. Time-course changes of relative *PCE* of the hybrid cells composed of glass-ITO/TiO₂/Sb₂S₃/HTL [HTL = P3HT/PEDOT:PSS (triangle), ZnPc (cross), or MoO₃ (circle)]/Au with UV cut filter at 63°C and 50% RH under 1 sun.

no irradiation of light. This result is probably ascribed to the acidic property of the diluted PEDOT:PSS solution, which tends to lower the cell performance.^{25,26} On the contrary, there was no lowering the *PCEs* after 1 d at 63°C and 50% RH in the dark both in the cases of ZnPc and MoO₃.

Effect of hole transporting layers (HTLs) on stability.—The durability test of the cells with UV cut filter was performed at 63°C and 50% RH under 1 sun as shown in Figure 2. *PCE* of P3HT/PEDOT:PSS decreased to the relative value of 10% after 100 h photo-irradiation. On the other hand, in the cases of ZnPc and MoO₃, *PCEs* kept constant until 300 h irradiation. However, that of MoO₃ started to decrease gradually after 300 h, while ZnPc indicated stable and 90% of *PCE* was retained after 500 h. TEM-EDX observations of the cross-sectional views of glass-ITO/TiO₂/Sb₂S₃/MoO₃/Au before and after the durability test for 576 h revealed that Sb and Mo diffused opposite directions one another (Figure 3). These diffusions during the durability test might affect the lowering of *PCEs*.

Effect of electron transporting layers (ETLs) on stability.—Two ETLs were utilized and compared in terms of durability for the

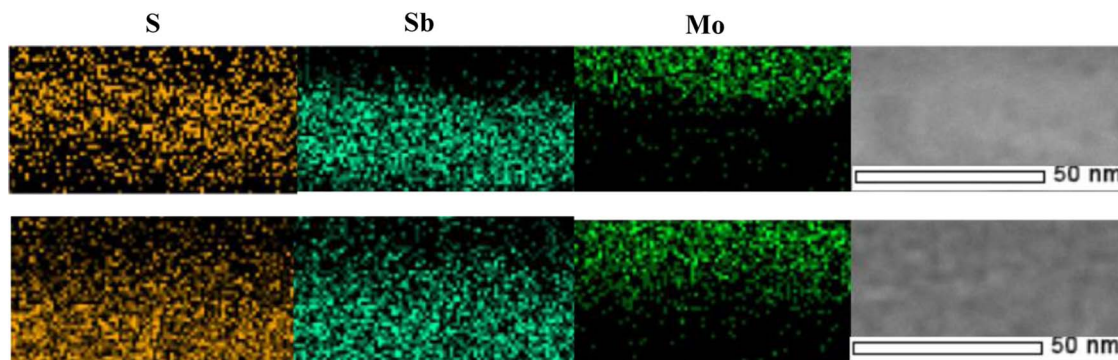


Figure 3. Cross sectional TEM images (right) and EDX images of S, Sb, and Mo elemental maps (left 3) of Sb₂S₃/MoO₃ layers of the hybrid solar cells composed of glass-ITO/TiO₂/Sb₂S₃/MoO₃/Au fresh after preparation (above), and after 576 h under 1 sun at 63°C and 50% RH (below). The thin film samples for the observations were prepared by FIB method after carbon coating and TEM and EDX have been operated with JEOL JEM-2010FEF at 200 kV.

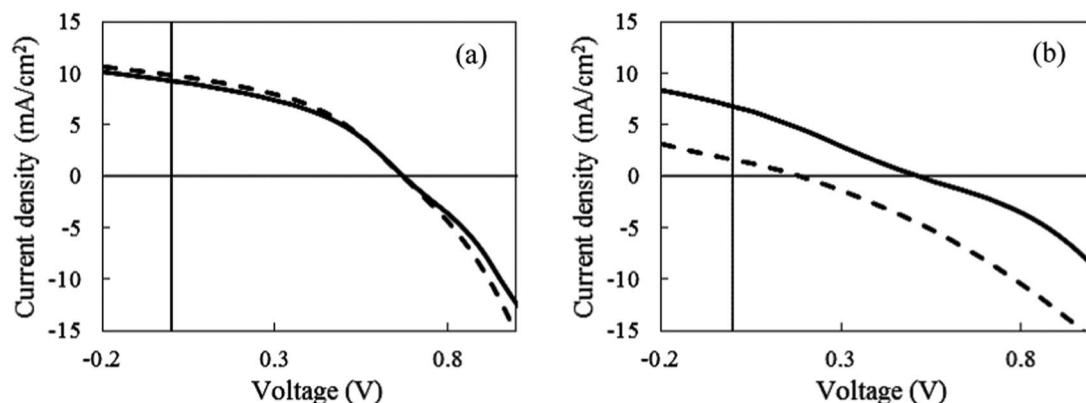


Figure 4. *J-V* curves of (a) glass-ITO/TiO₂/Sb₂S₃/ZnPC/Au, (b) glass-ITO/ZnO/Sb₂S₃/ZnPC/Au fresh after preparation (solid), and after 7 d at 63°C and 50% RH under 1 sun (broken).

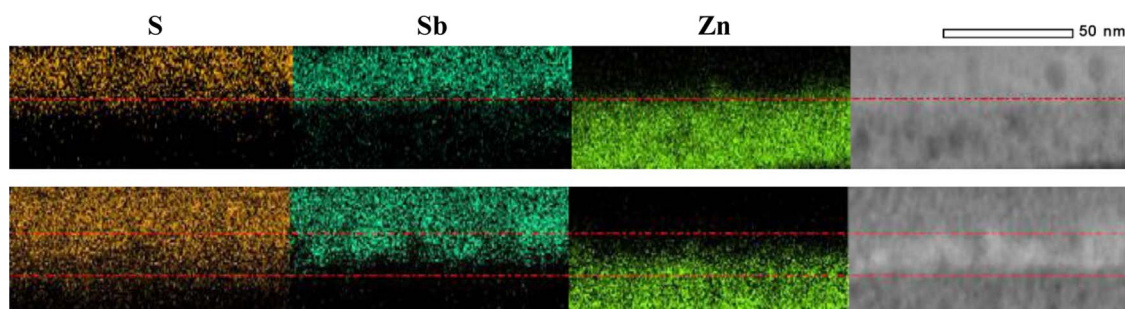


Figure 5. Cross sectional TEM images (right) and EDX images of S, Sb, and Zn elemental maps (left 3) of ZnO/Sb₂S₃ layers of the hybrid solar cells composed of glass-ITO/ZnO/Sb₂S₃/ZnPC/Au fresh after preparation (above), and after 7 d at 63°C and 50% RH under 1 sun (below). The thin film samples for the observations were prepared by FIB method after carbon coating and TEM and EDX have been operated with JEOL JEM-2010FEF at 200 kV.

Sb₂S₃-based hybrid solar cells with TiO₂ or ZnO nanoparticles as glass-ITO/TiO₂/Sb₂S₃/ZnPC/Au or glass-ITO/ZnO/Sb₂S₃/ZnPC/Au with UV cut filter at 63°C and 50% RH under 1 sun. The *J-V* curves of the initial photovoltaic performance and after 7 d and the time-course changes of relative *PCEs* through the durability test (Figure 4) indicate that almost constant stability of TiO₂-based cell and remarkable lowering of the *PCE* and lability of ZnO-based one. In particular, the fill factor (*FF*) and the series resistance (*R_s*) of glass-ITO/TiO₂/Sb₂S₃/ZnPC/Au had been improved as *FF* from 0.415 to 0.471, and *R_s* from 33 ohm cm² to 20 ohm cm² after 7 d, respectively. Therefore, using TiO₂ is effective to adjust the interface of the device under the conditions with UV cut filter at 63°C and 50% RH under 1 sun. On the other hand, it was found by TEM-EDX observations of the cross-sectional views of glass-ITO/ZnO/Sb₂S₃/ZnPC/Au (Figure 5) that initial distribution of S was well-corresponding with that of Sb, however, S diffused wider than Sb and migrated toward Zn after the durability test and presumably substitution of S of Sb₂S₃ for O of ZnO might occur and result in the formation of ZnS.

Effect of UV light irradiation on stability.—In order to investigate the effect of UV light irradiation, another durability test of glass-ITO/TiO₂/Sb₂S₃/ZnPC/Au without UV cut filter was performed at 63°C and 50% RH under 1 sun. The *J-V* curves of the initial photovoltaic performance (solid) and after 3 d (broken) were indicated in Figure 6. The relative *PCE* of 90% was retained for 1,500 h with UV cut filter, however the photovoltaic ability has almost been lost without the cut filter after 72 h. Decolorization was observed after the irradiation without the UV cut filter though the decolorization did not occur with the filter. Once the TiO₂ layer was removed from the cell, described as glass-ITO/Sb₂S₃/ZnPC/Au, there was no decolorization even when without using the UV cut filter. In this context, anatase

TiO₂ nanoparticles in this case act as the photocatalyst during the UV light irradiation²⁷ to oxidize and decompose Sb₂S₃, which resulted in the above decolorization of the cells. TEM-EDX observations of the cross-sectional views of colored (being not decolorized) site and decolorized site (Figure 7) indicated that the existence of S and O was confirmed at the colored site though only O was confirmed (*viz.*

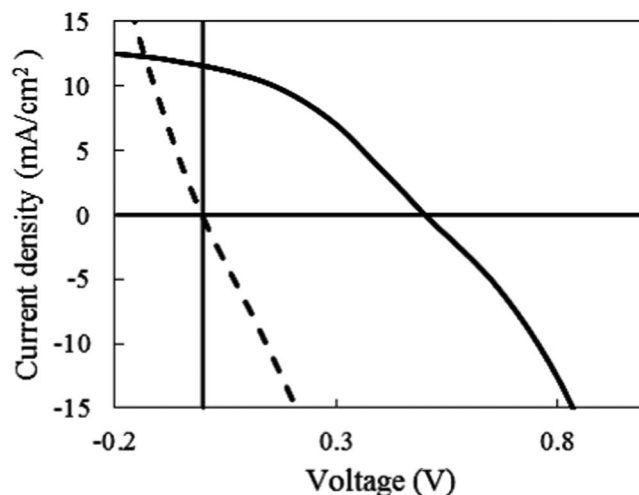


Figure 6. *J-V* curves of glass-ITO/TiO₂/Sb₂S₃/ZnPC/Au without UV cut filter fresh after preparation (solid) and after 3 d storage at 63°C and 50% RH under 1 sun (broken).

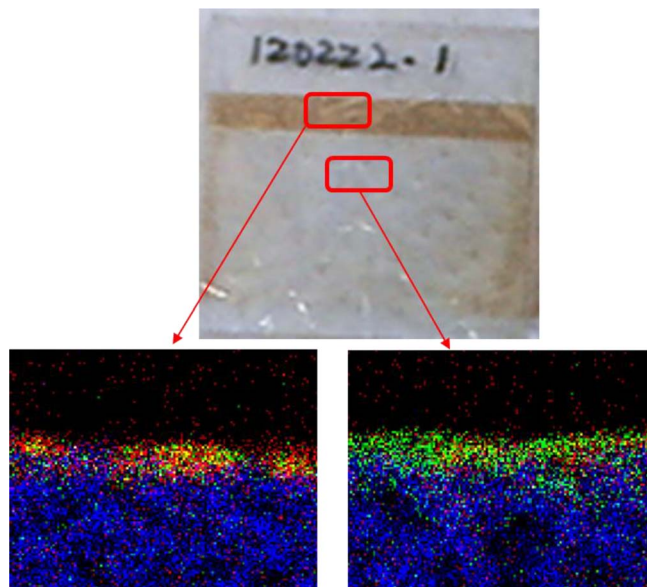


Figure 7. Cross sectional EDX images of S (red), Sb (green), and Ti (blue) elemental maps of colored site (left) and decolorized site (right) of ITO/TiO₂/Sb₂S₃ layers of the hybrid solar cells composed of glass-ITO/TiO₂/Sb₂S₃/ZnPC/Au without UV cut filter after 1 d at 63°C and 50% RH under 1 sun.

S was not detected) at the decolorized site. This is also supporting the oxidative decomposition of Sb₂S₃ by photoactivated TiO₂.

Summary

We prepared Sb₂S₃-based solar cells with ETL of TiO₂ or ZnO in addition to HTL of P3HT/PEDOT: PSS, ZnPC, or MoO₃ and compared their photovoltaic performance in terms of durability with encapsulation by using glass and UV cutoff films. Combination with ZnPC and TiO₂ has the highest durability with retaining the relative *PCE* of 90% under the conditions of 1 sun at 63°C at a relative humidity of 50% for 1,500 h. Effective suppression of the photoactivation of TiO₂ through UV light irradiation by using cut filter is essential to realize the long term stability and promising further extension for optimization of the photovoltaic performance.

Acknowledgments

This research was partially supported by The Ministry of Education, Culture, Sports, Science and Technology.

References

1. J. A. Chang, J. H. Rhee, S. H. Im, Y. H. Lee, H. J. Kim, S. I. Seok, M. K. Nazeeruddin, and M. Graetzel, *Nano Lett.*, **10**, 2609 (2010).
2. S. H. Im, C. S. Lim, J. A. Chang, Y. H. Lee, N. Maiti, H. J. Kim, M. K. Nazeeruddin, M. Graetzel, and S. I. Seok, *Nano Lett.*, **11**, 4789 (2011).
3. J. H. Heo, S. H. Im, J. Kim, P. P. Boix, S. J. Lee, S. I. Seok, I. M. Seo, and J. Bisquert, *J. Phys. Chem. C*, **116**, 20717 (2012).
4. Y. C. Choi, D. U. Lee, J. H. Noh, E. K. Kim, and S. I. Seok, *Adv. Funct. Mater.*, **24**, 3587 (2014).
5. N. Guijarro, T. Lutz, T. Lana-Villarreal, F. O'Mahony, R. Gomez, and S. A. Haque, *J. Phys. Chem. Lett.*, **3**, 1351 (2012).
6. H. Wang, T. Kubo, J. Nakazaki, T. Kinoshita, and H. Segawa, *J. Phys. Chem. Lett.*, **4**, 2455 (2013).
7. P. K. Santra and P. V. Kamat, *J. Am. Chem. Soc.*, **134**, 2508 (2012).
8. A. Kojima, K. Teshima, Y. Shirai, and T. Miyasaka, *J. Am. Chem. Soc.*, **131**, 6050 (2009).
9. M. M. Lee, J. Teuscher, T. Miyasaka, T. N. Murakami, and H. J. Snaith, *Science*, **338**, 643 (2012).
10. W. S. Yang, J. H. Noh, N. J. Jeon, Y. C. Kim, S. Ryu, J. Seo, and S. I. Seok, *Science*, **348**, 1234 (2015).
11. E. L. Gui, A. M. Kang, S. S. Pramana, N. Yantara, N. Mathews, and S. Mhaisalkar, *J. Electrochem. Soc.*, **159**, B247 (2012).
12. D. H. Kim, S. J. Lee, M. S. Park, J. K. Kang, J. H. Heo, S. H. Im, and S. J. Sung, *Nanoscale*, **6**, 14549 (2014).
13. Y. C. Choi and S. I. Seok, *Adv. Funct. Mater.*, **25**, 2892 (2015).
14. R. Gonzalez-Lua, J. Escorcia-Garcia, D. Perez-Martinez, M. T. S. Nair, J. Campos, and P. K. Nair, *ECS J. Solid State Sci. Technol.*, **4**, Q9 (2015).
15. C. P. Liu, Z. H. Chen, H. E. Wang, S. K. Jha, W. J. Zhang, I. Bello, and J. A. Zapien, *Appl. Phys. Lett.*, **100**, 243102 (2012).
16. T. Oku, T. Yamada, K. Fujimoto, and T. Akiyama, *Coatings*, **4**, 203 (2014).
17. S. Panigrahi, T. Calmeiro, R. Martins, D. Nunes, and E. Fortunato, *ACS Nano*, **10**, 6139 (2016).
18. T. Minami, Y. Nishi, and T. Miyata, *Appl. Phys. Express*, **9**, 052301/1-052301/4 (2016).
19. A. Kay and M. Graetzel, *Chem. Mater.*, **14**, 2930 (2002).
20. S. J. Moon, Y. Itzhaik, J. H. Yum, S. M. Zakeeruddin, G. Hodes, and M. Graetzel, *J. Phys. Chem. Lett.*, **1**, 1524 (2010).
21. K. Tsujimoto, D. C. Nguyen, S. Ito, H. Nishino, H. Matsuyoshi, A. Konno, G. R. A. Kumara, and K. Tennakone, *J. Phys. Chem. C*, **116**, 13465 (2012).
22. J. H. Li, J. Huang, and Y. Yang, *Appl. Phys. Lett.*, **90**, 173505 (2007).
23. A. S. Subbiah, A. Halder, S. Ghosh, N. Mahuli, G. Hodes, and S. K. Sarkar, *J. Phys. Chem. Lett.*, **5**, (2014).
24. W. J. E. Beek, M. M. Wienk, M. Kemerink, X. Yang, and R. A. J. Janssen, *J. Phys. Chem. B*, **109**, 9505 (2005).
25. O. Synooka, F. Kretschmer, M. D. Hager, M. Himmerlich, S. Krischok, D. Gehrig, F. Laquai, U. S. Schubert, G. Gobsch, and H. Hoppe, *ACS Appl. Mater. Interfaces*, **6**, 11068 (2014).
26. B. Roth, G. A. R. Benatto, M. Corazza, R. R. Sondergaard, S. A. Gevorgyan, M. Jorgensen, and F. C. Krebs, *Adv. Energy Mater.*, **5**, 1401912/1 (2015).
27. X. Wang, Z. Li, J. Shi, and Y. Yu, *Chem. Rev.*, **114**, 9346 (2014).